Deflectometry challenges interferometry – the competition gets tougher!

Christian Faber*, Evelyn Olesch, Roman Krobot, Gerd Häusler
Institute of Optics, Information, and Photonics
Friedrich-Alexander University Erlangen-Nuremberg
Staudtstraße 7/B2, D-91058 Erlangen, Germany

ABSTRACT

Deflectometric methods that are capable of providing full-field topography data for specular freeform surfaces have been around for more than a decade. They have proven successful in various fields of application, such as the measurement of progressive power eyeglasses, painted car body panels, or windshields. However, up to now deflectometry has not been considered as a viable competitor to interferometry, especially for the qualification of optical components. The reason is that, despite the unparalleled local sensitivity provided by deflectometric methods, the *global height accuracy* attainable with this measurement technique used to be limited to several microns over a field of 100 mm. Moreover, *spurious reflections* at the rear surface of transparent objects could easily mess up the measured signal completely. Due to new calibration and evaluation procedures, this situation has changed lately. We will give a comparative assessment of the strengths and – now partly revised – weaknesses of both measurement principles from the current perspective. By presenting recent developments and measurement examples from different applications, we will show that deflectometry is now heading to become a serious competitor to interferometry.

Keywords: specular freeform surfaces, deflectometry, PMD, slope sensitive methods, global accuracy, calibration

1. INTRODUCTION

When it comes to accurate contact-free measurements of specular surfaces, interferometry has been the only viable 'game in town' for more than a century. This is not surprising, as this measurement principle combines two important advantages: The relationship between the *target quantity* (the surface height $z(x,y)$) and the *primary measurand* (the interference phase $\varphi(x,y)$) is quite straightforward (2), and the precision and accuracy attainable with this technique is extremely high. The latter is due to the fact that the dimensional scale determining the measurement uncertainty is given by the wavelength λ – or rather fractions of λ when using well-established phase evaluation techniques[1].

However, even today the task of measuring arbitrary freeforms lets interferometry often come up against its limits: The need for compensation optics or CGHs[2] renders this approach quite inflexible and costly. Furthermore, providing an appropriate system calibration quickly becomes an intractable task due to retrace errors[3]. Finally, integrating interferometric techniques into a harsh production environment is an extremely challenging endeavour: Interferometric setups tend to be prone to *coherent noise* (easily caused by contaminations or scratches on the lens elements) and are typically very sensitive against vibrations and environmental influences like pressure and temperature fluctuations.

Therefore, scientists have started early to look for alternatives. One idea is to exploit the special way the probing radiation interacts with specular surfaces: instead of scattering, there is a *directed deflection* of the incident light. By measuring the *amount of deflection*, information about the surface can be obtained. This approach is quite different from the interferometric paradigm: Whereas interferometry relies at its heart on the *wave nature of light* (manifesting itself by the fact that the gauge of the measurement principle is given by the wavelength λ), this is not the case for deflectometry. Although the wave nature of light ultimately limits the attainable accuracy for deflectometry as well, it does *not* define its dimensional scale, which is given by purely geometric considerations. Moreover, deflectometry is a fundamentally *incoherent* technique.

Early applications of this principle are the *Foucault Knife Edge test*[4] (providing rather qualitative data) or the *Shack-Hartmann sensor*[5,6] (yielding quantitative values on a discrete set of sampling points). A more recent implementation, capable of providing both quantitative *and* pixel-dense full-field data, is the technique of *Phase Measuring Deflecto-*

*christian.faber@physik.uni-erlangen.de; phone +49 9131 85 28385; fax +49 9131 13508; www.optik.uni-erlangen.de/osmin/

metry (PMD) introduced by Häusler et al[7,8]. This method is based on the *reflection grating principle* proposed by Ritter and Hahn[9], enhanced by the introduction of a (phase-shifted) *sinusoidal pattern* rather than a binary grating. This accounts for the fact that in deflectometry, the observed structured pattern usually has to be placed out-of-focus. Other implementations based on the same principle are – without claiming to be exhaustive – known as *Rasterreflektions-verfahren*[10,11], *Structured-Lighting Reflection*[12,13], *Fringe Reflection*[14], *Verfahren Inverser Muster*[15], *Shape from Specular Reflection*[16], *Computerized Reverse Hartmann Test*[17], or simply by the term *Deflectometry*[18].

The biggest advantage of all these approaches – aside from an unparalleled dynamic range and the lack of coherent noise – is that when applied properly, there is *no retrace error*, and no need to probe the surface under test at normal incidence. This will be elaborated further in the following sections.

Having these advantages in mind, some propositions have been made several years ago, claiming that the new deflectometric techniques may have the potential to rival interferometry on its own turf of high-precision measurements for specular surfaces – especially for the case of aspheres and freeforms[19,20,21]. However, at that time, these claims still had to be filed under "visionary", for deflectometry had its own specific shortcomings as well: Due to the fact that the primary measurand is given by the surface slope, low spatial frequencies of the object shape are suppressed and – in presence of calibration errors – essentially lost. Therefore, the global height accuracy used to be limited to several microns over a field of 100 mm – whereas the *local* sensitivity could easily reach the range of a few nanometers. Furthermore, spurious reflections at the rear side of transparent specimens could quickly mess up the measured signal completely.

Over the past few years, considerable progress has been made to overcome these limitations: Due to new calibration and evaluation procedures, the measurement error could be reduced down to the sub-micron range on a field of view of 100 mm, still with room for improvement[22,23]. Artefacts from spurious reflections could be suppressed effectively[24-26]. Thus, deflectometry now starts to become a serious competitor for interferometry in the sub-micron regime (but not for the nanometer regime, so far). In the following sections, the recent developments are presented and measurement examples from different applications are shown. A more detailed description can be found in the PhD thesis of the author[27].

2. PECULIARITIES OF SPECULAR SURFACES

Before we start, it is a good idea to briefly review why specular surfaces should be so difficult to measure. After all, the absence of a micro-roughness within the resolution cell of the measurement system (which is the very definition of being "specular") should rather be considered a blessing, as it prevents the formation of unwanted stochastic interferences – i.e. speckles – in the observation plane. According to the Rayleigh criterion, this is assured if the local height variations within the resolution cell are considerably lower than $\lambda/8$, resulting in a relative phase variation of less than $\lambda/4$ if the surface is probed in normal reflection. However, the better this criterion is met, the more the scatter indicatrix of the surface will converge towards a *delta function*, where the angle of reflection is equal to the angle of incidence – this being the *only* direction into which light is emitted. Although this well-known fact may appear trivial at first sight, it still has some severe consequences:

A specular surface is actually *invisible* and should rather be considered as part of the imaging system! Due to the lack of scattered light, we don't "see" the surface itself – we rather see a (distorted) image of the surrounding light sources (resp. luminance distribution). It should be noted that when we touch the top of the water tap in the bathroom in the morning, our brain already accomplishes an almost incredible feat, as it subconsciously infers the correct position of the tap's surface just from the way the tiles of the bathroom walls appear distorted in the reflected image. Even before we are fully awake, we have successfully performed a complete inverse ray tracing computation in our head!

2.1 The aperture problem

The issue described above has one particularly unfavorable consequence when it comes to measurement applications:

If we want to capture some light with an observation system mounted at a specific location, we have to make sure that there is a *luminous source at the right position*, whose rays are reflected by the specular surface into the observation pupil. If the shape and the slope of the object surface are unknown, there are only two options to achieve this: Either we use a very *large observation aperture* – or we use a *spatially extended light source*, at the expense of not knowing in advance which particular part of the light source will be used for the final imaging. This is called the "aperture problem" of specular surfaces (see fig.1).

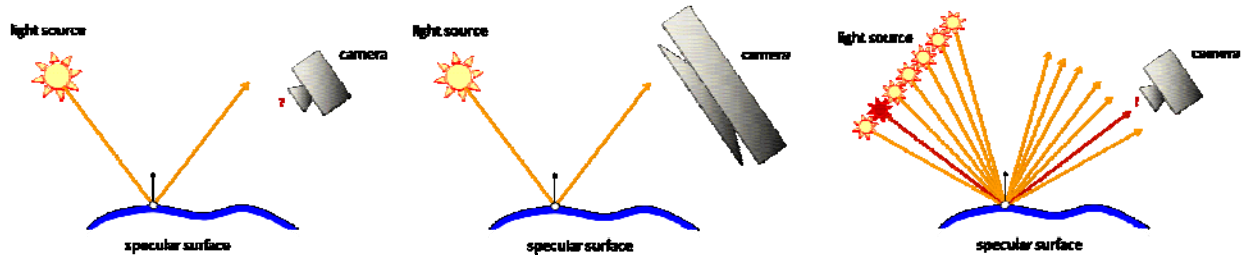

Figure 1. Left: The "aperture problem" of specular surfaces[27]. Center: Solving the aperture problem by using a *large entrance pupil* for the observation system (costly). Right: Solving the aperture problem by using an *extended light source*. A third solution (for a *known* surface) would be to "put the light source at the right position" (i.e. just using the dark colored "sun" in the right sketch), corresponding to the concept of *null-testing* (see section 3.1).

2.2 The dynamic range problem

The majority of specular surfaces to be measured are used for applications in *optics*. Particularly for imaging optics, the target accuracy of the surface shape is often given by the Rayleigh criterion, tolerating wavefront aberrations up to $\lambda/4 \approx 100\text{nm}$. Consequently, the acceptable measurement uncertainty for these applications typically lies in the range of $\delta z \approx 10\text{nm}$. At the same time, the sag of an optical element to be tested can easily be $\Delta z \approx 10\text{mm}$ or more. This results in a *required dynamic height range* for the measurement system of

$$D = \frac{\Delta z}{\delta z} = \frac{10mm}{10nm} = 10^6 \tag{1}$$

This is very difficult to achieve with analog systems, as it requires *20 valid (significant) bits after AD conversion*!

We will see in the next section how the two competing measurement principles – interferometry and deflectometry – are dealing with these two problems (aperture and dynamic range), which are inherent to all optical measurements on specular surfaces.

3. REVIEW OF THE MEASUREMENT PRINCIPLES

In this section, the basic measurement principles of both interferometry and deflectometry are briefly reviewed. We will pay special attention to the specific signal generation and information encoding processes of both measurement techniques, as they are quite different from each other, resulting in very different properties and behavior with respect to robustness and measurement accuracy[27].

3.1 Interferometry

The basic principle of interferometry has been well known for more than a century. In this paper, we will restrict ourselves to the case of classical *homodyne interferometry*, as the testing of optical surfaces requires a full-field measurement, and heterodyne interferometry is typically used for point measurements only.

The standard setups applied for optical shop testing are the *Twyman-Green*, the *Fizeau,* and the *Mach-Zehnder interferometer*[3,28]. In each case, the quantity of interest – the surface height $z_{obj}(x,y)$ – is encoded in the *relative interference phase*

$$\varphi(x,y) = k(x,y) \cdot \frac{2\pi}{\lambda} \cdot \left(\Delta z(x,y) \bmod \left(\frac{\lambda}{k(x,y)} \right) \right) \tag{2}$$

with $\Delta z(x,y) = z_{obj}(x,y) - z_{ref}(x,y)$ denoting the height difference between the object and the reference surface. The geometry factor k depends on the specific layout resp. incidence angles of the setup and would be $k=2$ for a reflective null-test setup using normal incidence. For the sake of simplicity, we will neglect this factor in the upcoming discussion.

Thus, the *primary measurand* of interferometry is given by the (relative) *object height modulo λ, scaled in units of λ* (except for the special case of shearing interferometry, where $z_{ref}(x,y) \sim z_{obj}(x+s_x,\ y+s_y)$). This has some important ramifications:

- Random errors of the interference phase result in a *random height error*

$$\delta z \approx \frac{\lambda}{Q} \tag{3}$$

  with a *quality factor Q* determined by the number of phase shifts *N*, interference contrast *K* and the signal-to-noise ratio *SNR* of the recorded intensity data[29,30]: $Q \sim \sqrt{N} \cdot K \cdot SNR$.

- Deviations in the *reference surface* directly affect the *trueness* of the measurement, even if they are only of the order of fractions of λ.

- The same (with respect to *precision* rather than trueness) holds for *fluctuations of the optical path length* in the non-common part of the beam path, induced by pressure or temperature variations, or by vibrations of the setup.

- The wavelength λ also sets the scale for tolerated *deviations* in the optical path length, again affecting the trueness of the measurement data. Such deviations can for example be induced by part-dependent aberrations of the lens system, as the exact path followed by the light back through the interferometer (after being reflected at the test surface) depends on the specific specimen if the light is not probing the surface exactly at normal incidence. This problem is called the *retrace error* of interferometry.

- The "mod λ" *encoding operator* may in principle be regarded as beneficial, as it removes redundancy from the data: The useless information about the stand-off distance is removed from the measurement, and the spatial spectrum of the measurand (which tends to drop like $\sim 1/\nu^{\alpha}$ with α in the order of unity for typical surfaces) is effectively whitened[27]. This can be understood easily by bringing to mind that the modulo-operator is acting as a very effective "correlation killer", which is exactly the reason for its wide-spread use in pseudorandom number generation. More details and explicit examples can be found in reference [27]. However, this "elimination of redundancy" comes at a high price: The encoding operator is *highly non-linear*, as it introduces new (*artificial*!) high spatial frequencies where there have been none in the original signal. This non-linearity makes it hard to ensure a robust *decoding* in the presence of noise. It is a well known fact that the unwrapping process in interferometry can introduce strong artifacts – and even may break down completely – for low signal-to-noise ratios. Furthermore, the additional high spatial frequencies introduced by the modulo-operator have to be *resolved by the measurement apparatus*.

The combination of the points discussed above (and particularly the "mod λ"-problem) results in severe repercussions when using interferometry for measurement purposes: Except for the special case of rotational symmetry[31], or very elaborate setups[32], the **applicability of interferometry is essentially limited to null-testing**, i.e. to determining only the *deviation* of the surface height (resp. object wavefront) *from its expected shape* rather than the shape itself. For aspheres and freeforms, this is usually done by implementing appropriate *compensation optics* or *CGH*s as null lenses.

On the positive side, this restriction is so severe that it automatically solves the two "specular-surface-problems" described in section 2 as well: If we confine ourselves to null-testing, the *dynamic range problem* is eliminated by definition, as the actual height extent (resp. sag) of the specimen does not have to be covered by the measurement range any more. Furthermore, if the deviation of the surface from the expected shape is not too big, the object under test will be *probed at normal incidence*, thus getting rid of the *aperture problem* as well (while at the same time keeping the retrace error under control).

The drawback of null-testing is of course that the need for compensation optics renders this method very inflexible and costly, particularly for small batch sizes. In addition, a tedious alignment of the test specimen is required to actually keep the deviations sufficiently small.

3.2 Deflectometry

As described in section 1, the underlying idea of deflectometry is to *measure the amount of beam deflection* induced by the interaction with the specimen under test. This can be done *actively*, using a light ray with a known source as probing device and determining the deflection angle θ by a suitable position sensitive detector (PSD, CCD or CMOS sensor) at a known distance *d* (see fig. 2 left). This approach has been successfully used for several implementations[33,34]. However, it only allows for a *pointwise* measurement and therefore requires an *x,y-scanning* (or the use of multiple known sources in parallel, restricting the measurement to a discrete sampling grid[35]).

Alternatively, the deflectometric principle can be implemented *passively*, using a spatially extended light source and *encoding* the different ray angles accordingly (for example by structuring the light source in an appropriate way). In this case, an *imaging device* focused on the specimen can be used on the detector side, allowing for a parallel full-field measurement. The same principle lies at the heart of the Foucault knife edge test[4]. For passive deflectometry, the specific location resp. part of the light source observed by a given pixel is *unknown* prior to the measurement and constitutes the very information obtained by the measurement process. Therefore, it is helpful to think in terms of *sight rays* rather than *light rays* for passive deflectometry: The object is "probed" by the chief rays of the observation system. This is depicted in the right part of figure 2.

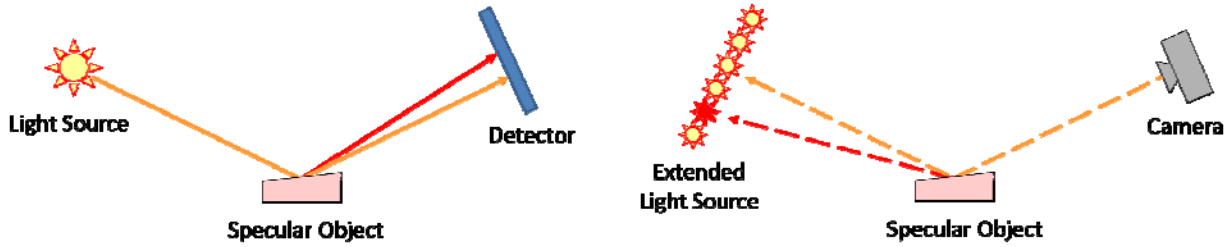

Figure 2. Basic principle of deflectometry[27]. Left: Active deflectometry, probing the object with a light ray emerging from a known source location. The deflection angle is measured by a position sensitive device on the detector side. Right: Passive deflectometry, probing the object with "sight rays", i.e. chief rays of an imaging system. An extended light source is used. The deflection angle is determined by encoding different locations on the light source differently.

A quantitative implementation of the passive deflectometric principle is given by the *Phase Measuring Deflectometry* technique (PMD)[7,8]. The basic principle is sketched in figure 3: A spatial light modulator capable of displaying different sinusoidal gratings is used as light source (either directly by using an LCD/TFT monitor, or by projecting the structured pattern onto a ground glass). This light source (or "screen") is observed by a calibrated camera via the object surface. By an appropriate phase shifting, the specific location on the screen "seen" by each single observation pixel can be determined with very high accuracy.

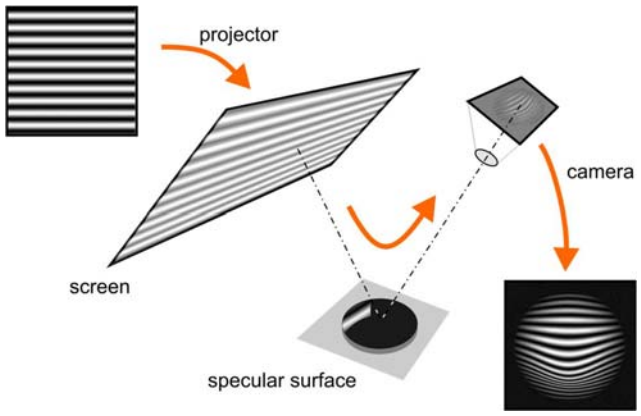

Figure 3. Basic principle of Phase Measuring Deflectometry (PMD). An extended light source structured with a sinusoidal luminance pattern is observed using the surface of the object under test as a mirror. The topography of the surface slopes is encoded in the distortion of the observed fringe pattern. Image courtesy of M.C. Knauer[8,40].

Using additional information about the specific location of the specimen, the *local surface normal* (and therefore the local slope of the specimen) can be inferred. The required distance information (needed to solve the so-called "height ambiguity" or "regularization problem" of PMD[36,37]) can either be provided by an additional (external) measurement of one surface point in conjunction with an appropriate iteration process[12,13], by displacing the screen by a known distance and repeating the measurement[10,11], or by using a second camera exploiting a stereo-like approach[38-40]. Alternatively, the screen can be shifted virtually to infinity by placing it into the focal plane of a large lens (so-called "direction coded deflectometry" RCD[41,42]). A well-established technique is to determine *one point* of the object surface using the Stereo-Deflectometry method introduced by Knauer[38-40], and to apply the iteration approach[12,13] for the rest of the surface. For surfaces that are only partially specular, a combination with a shape from shading approach can be used[43]. Comprehensive overviews of the different options to solve the height ambiguity problem are given by Kaminski[44] and Werling[37].

Regardless of how the height ambiguity is solved, it is obvious that PMD is primarily sensitive to the local *slope* of the surface under test. As in the case of interferometry, this special choice of primary measurand has some important ramifications – albeit quite different ones from those discussed in section 3.1:

- The random errors contained in the raw data of the measurement now affect the *slope* rather than the height of the object. It has been shown by Häusler et al.[7,8,40] that for an optimized setup, the uncertainty $\delta\alpha$ of the slope angle α (which is linked directly to the uncertainty $\delta\theta$ in determination of the deflection angle θ via $\delta\alpha=1/2\ \delta\theta$) is coupled to the *lateral resolution* δx of the observation system by an *uncertainty relation*:

$$\delta x \cdot \delta\alpha \geq \frac{\lambda}{Q} \tag{4}$$

  with Q again denoting a *quality factor* dominated by the *SNR* of the recorded intensity data. This inequality becomes an equation in case of a *diffraction limited setup*, applying an optimized spatial frequency for the fringes (which has to be adjusted to the *f/#* of the observation system). This leads to an estimate of the detectable *local height variation* δz *within the resolution cell* δx which is remarkably similar to the expression for the random height error of interferometry described in section 3.1:

$$\delta z \approx \delta x \cdot \delta\alpha \sim \frac{\lambda}{Q} \tag{5}$$

  In particular, this relation reveals that deflectometry is capable of detecting *local height variations* in the *nanometer range*, as quality factors of $Q\approx500$ can easily be achieved with sufficiently long exposure times and bright light sources.

- In contrast to interferometry, deflectometry does not have a height reference that the surface figure is put in relation to. However, the deflection angle θ which yields the local surface slope $\alpha=1/2\ \theta$ is measured relative to the "known" directions of the incident probing rays. Therefore, the *trueness of the slope data* will be affected by the *accuracy of the system calibration*.

- As the primary measurand is determined by $\left(\partial z/\partial x, \partial z/\partial y\right)$ rather than $z \bmod \lambda$, the *sensitivity to environmental influences* is quite different compared to interferometry: Pressure and temperature variations will still affect the measurement – but now only by virtue of their *spatial gradients*[27] $\nabla P(\vec{r}), \nabla T(\vec{r})$. Moreover, the amount of error induced by these fluctuations does not scale with the optical path length resp. the wavelength λ anymore and can therefore be controlled and adjusted by the geometry and spatial dimensions of the setup! This is particularly important for the sensitivity against vibrations, which now allows for *vibration amplitudes of several* λ without destroying the measurement information. Furthermore, the spatial incoherence provided by the extended light source avoids coherent artifacts in the measurement signal, rendering deflectometry very *robust against contaminations*.

- As the dimensional scale of a deflectometric setup is *not* set by the wavelength λ, this measurement principle can easily be adjusted for different object sizes and is therefore remarkably *scaleable over several orders of magnitude*[21].

- For conventional (non-microscopic) deflectometric setups, the observation pupil can be chosen rather small compared to the overall angular spectrum of the probing rays. As these probing rays just propagate through free space, deflectometry does – to a very large extent – *not suffer from retrace errors*[27]. In particular, the object surface *does not have to be probed at normal incidence.*

- Finally, deflectometry also provides a *whitening of the object spectrum*, thus increasing the information efficiency by *removing redundancy from the measurement data.* However, in contrast to interferometry, this is achieved by using a (linear) *derivative operator* rather than a (non linear) modulo operator[27]. As a consequence, deflectometry does *not* introduce new (artificial) high spatial frequencies to the measurement signal – it rather amplifies only those high spatial frequencies that have been present in the object spectrum in the first place. Furthermore, the decoding procedure (numerical integration) is considerably more robust than in the case of interferometry.

What does this entail for the two "specular surface problems" described in section 2?

The "*aperture problem*" is readily solved by applying the approach shown in the right sketch of figure 1 (using an extended light source). Mind the fact that this solution is not that easily available for interferometry, as it involves an a priori unknown source location. One interferometric method coming close to this approach is the so-called "*tilted wave interferometry*" introduced by Garbusi et al.[32].

The "*dynamic range problem*" is solved by measuring the *derivative* of the height function rather than the object surface $z(x,y)$ itself. For some applications (like the quality assurance of progressive power eyeglasses), the surface shape is not even needed, as the quantity of interest (in this case the local refractive power) may directly be determined by (higher order) derivatives of the surface function rather than by the height data.

Remarkably, both "specular surface problems" are solved *without the need to probe the object surface at normal incidence*. As a consequence, even for arbitrary freeforms, **deflectometry is not limited to null-testing**. This is a considerable – and very fundamental – advantage.

4. SHORTCOMINGS OF DEFLECTOMETRY

Looking back at the two "bullet point lists" presented above, one may wonder why interferometry has not been replaced by deflectometry a long time ago. The reason is that deflectometry also has some specific shortcomings which in the past proved to be prohibitive when trying to use deflectometric methods for the measurement and qualification of optical components:

- Unfortunately, the local height sensitivity in the nanometer range suggested by equation (5) cannot simply be transferred to (resp. be interpreted as) a *global height uncertainty* valid for all measurement points regardless of their lateral distance. The reason is that the derivative operator which – as explained in the previous section – is used for signal encoding effectively *suppresses low spatial frequencies of the object structure*. As soon as the measurement errors introduced by the setup for different spatial observation points are *correlated*, the final result will be dominated by these errors rather than by the object signal! This unfortunate situation is exactly what happens if there is a *miscalibration* of the measurement system. Therefore, all deflectometric setups are **extremely prone to calibration errors** – far more than it is the case for interferometry.
- A large number of objects with optically smooth surfaces to be tested are *transparent*. Consequently, there will be additional reflexes of the probing radiation occurring at the rear surface of the specimen under test. While this problem can be addressed in interferometric test setups by properly adjusting the coherence length of the light or by introducing additional phase shifts[45], the only remedy for deflectometric measurements in the past has been to **blacken and roughen the rear surface** (or to immerse the rear surface into a refractive index adapted material). This is of course prohibitive for non-destructive testing directly on the shop floor.

Throughout the last years, there has been considerable progress with respect to both these limitations. This will be elaborated further in the following sections.

5. NEW SYSTEM CALIBRATION

The conventional calibration of a deflectometric setup is done by applying standard photogrammetric methods like resection and bundle adjustment, and consists of three separate (but nevertheless interdependent) steps[36,40]:

First, the exact relation between the local phase value of the sinusoidal pattern and the corresponding location on the screen has to be determined. This step is called *pattern calibration*. Due to a possible distortion of the pattern, this relationship might be non linear. Second, each observation pixel P has to be associated with its corresponding "sight ray", defined by the set of points in 3d-space which are imaged onto pixel P. This step is called *camera calibration*. Finally, everything has to be transferred into one common coordinate system by appropriate resection procedures (the so-called *geometry calibration*). The basic principle is depicted in figure 4.

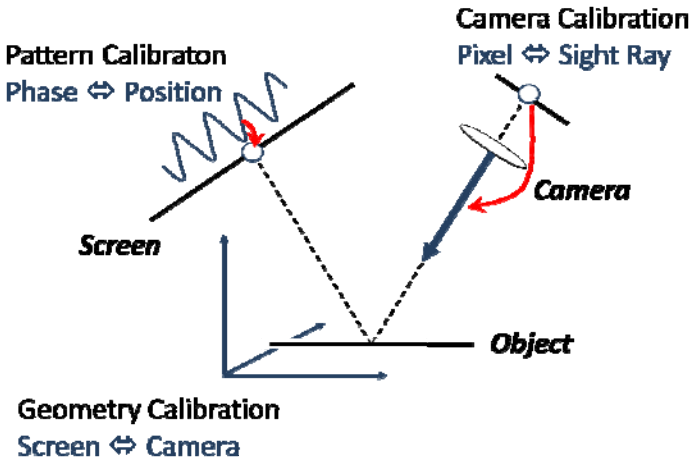

Figure 4. Basic principle of the conventional calibration procedure for a deflectometric setup[27]. The calibration is divided into different steps corresponding to the different sub-components of the setup.

Although quite successful in the past, this calibration concept turned out to have some drawbacks when it comes to high accuracy demands:

Due to unavoidable uncertainties in the photogrammetric measurements that are required for the calibration procedure, the set of calibration parameters determined by this process for the different sub-systems usually tended to be *inconsistent* (to a certain extent). As a consequence, the calibration model could describe the setup with limited fidelity only, resulting in global height deviations of more than 3µm on a field of view of 80mm. Figure 5 shows the typical measurement error obtained on a planar λ/10-mirror with a PMD setup calibrated this "conventional" way:

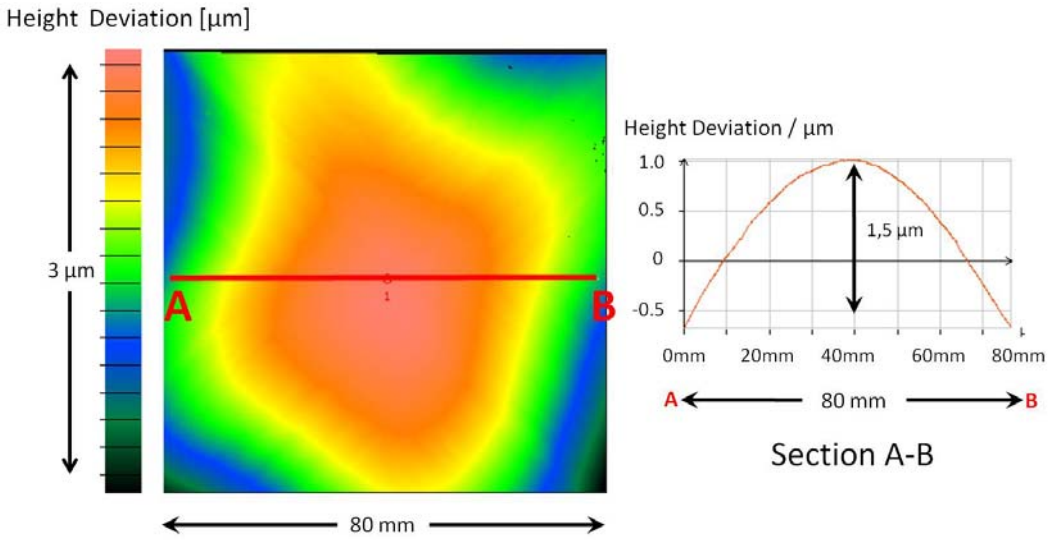

Figure 5. Global height deviation of the measurement of a planar λ/10-mirror, using a setup that has been calibrated by the conventional procedure described above[27].

To get rid of these limitations, a new calibration concept has been introduced, transferring the basic idea of a *self calibration* (applied for example in photogrammetric bundle adjustment on marker plates) to the case of a featureless specular (i.e. invisible!) object[22,23,27]. Instead of dividing the setup into different (possibly inconsistent) components, all calibration parameters needed to describe the course of the probing rays within the measurement volume are determined by *one global optimization process*. This is done using multiple PMD-measurements of the same calibration device (e.g. a planar mirror or a precision sphere), which is shifted and rotated between the measurements. Thus, with each new measurement, only 6 (or fewer!) new unknowns are introduced (corresponding to the 6 degrees of freedom of a rigid

body motion), whereas millions of new data values are obtained (when using a megapixel camera). As in the case of a bundle adjustment, one finally ends up with an overdetermined inverse problem that can be solved by appropriate optimization algorithms. Figure 6 shows the same measurement as figure 5, after the system has been calibrated using the new procedure. The measurement uncertainty has been reduced by a factor of 6 below 0.5µm on a field of view of 80mm.

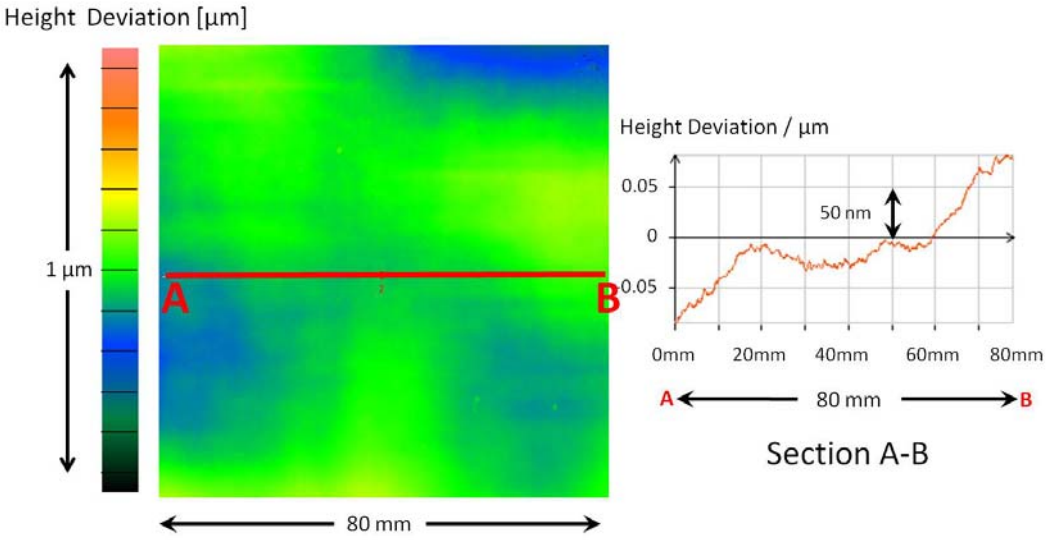

Figure 6. Global height deviation of the measurement of a planar λ/10-mirror, using a setup that has been calibrated with the new procedure[27].

As a nice by-product, the new method only requires standard PMD measurements without the need of marker detection or label assignment. Therefore, it can be performed easily in the field by any operator capable of conducting "conventional" measurements.

6. AVOIDING THE BACK SIDE REFLEX

The problem of the back side reflex is depicted in figure 7: For a transparent object, each observation pixel *P* receives an incoherent *superposition* of signals originating from two separate source locations 1, 2 on the screen. The resulting beat signal cannot be processed by the conventional evaluation procedure.

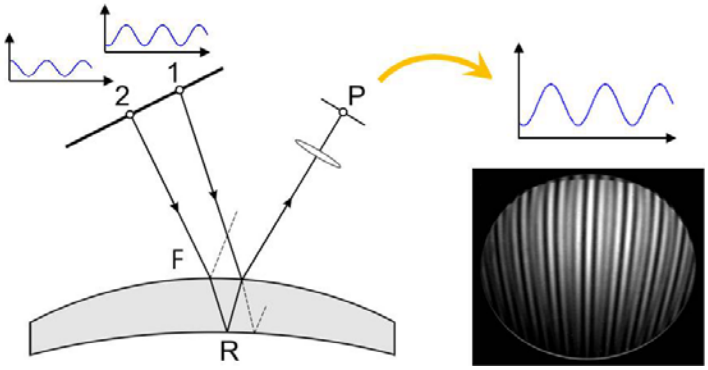

Figure 7. Problem of the back side reflex[27]: For transparent objects, each observation pixel *P* receives an incoherent superposition of multiple signals, reflected at the front (*F*) and the rear (*R*) surface of the specimen.

The perturbation induced by this superposition renders a conventional measurement impossible as soon as the relative modulation of the parasitic rear surface signal exceeds ~0.5% compared to the useful front surface signal. This threshold is reached quickly for almost all practical applications using transparent objects.

Several solution approaches have been proposed for this problem[24]. One option is an *a-posteriori algorithmic signal separation*. The additional information required for this approach can be provided using *multiple fringe frequencies*. The feasibility of this solution has been demonstrated successfully[25,27]. However, the non-linear inverse problem that has to be solved in this context turned out to be *ill-conditioned* along one-dimensional curve structures on the object (so-called "*pathological lines*"). These are exactly those points on the object where the signals from the front and the rear surface are very close to each other and therefore hard to separate. As shown in figures 8 and 9, the course of these pathological lines depends on the specific geometry of the setup, allowing for a solution using multiple view directions.

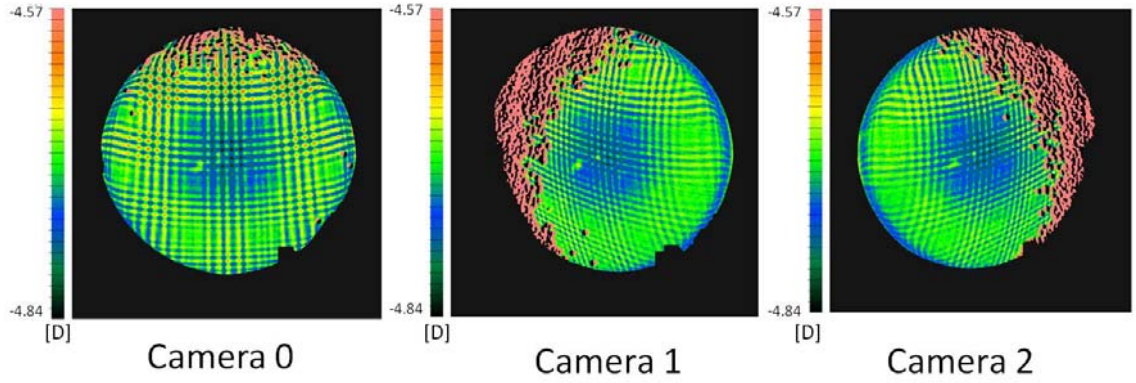

Figure 8. Perturbations in the curvature maps of a concave lens induced by the back side reflex for conventional PMD measurements using three different viewing directions[27]. The relative modulation of the parasitic back side signal is 3.2%.

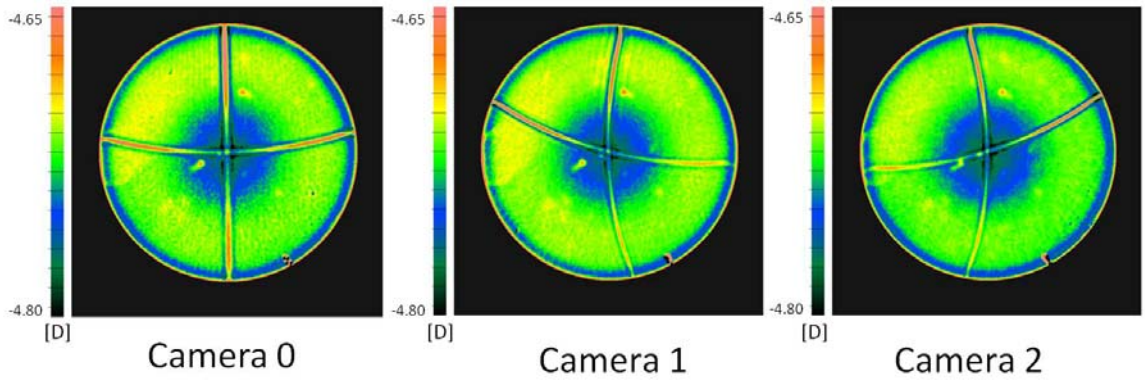

Figure 9. The same specimen as in Fig. 8, evaluated using the multifrequency method[27]. Except for one-dimensional "pathological line" structures, the algorithmic signal separation has been successful.

Alternatively, the problem can also be solved by *suppressing* the back side reflex completely, using UV instead of visible light[26]. However, as no suitable spatial light modulators are available in the required wavelength range, a new method had to be introduced, using a *moving line* rather than a phase-shifted sinusoidal pattern[26,27] (the concept of using a moving line for deflectometry has been developed and demonstrated independently by a group in Arizona, using visible light for applications on mirrors and solar concentrators[17]). It has been shown[27] that the achievable accuracy of this so-called *Line-Shift Deflectometry* is guided by the same uncertainty relation (4) as its phase-shifting "cousin". The first prototype of a UV-line-shift deflectometric setup is shown in figure 10.

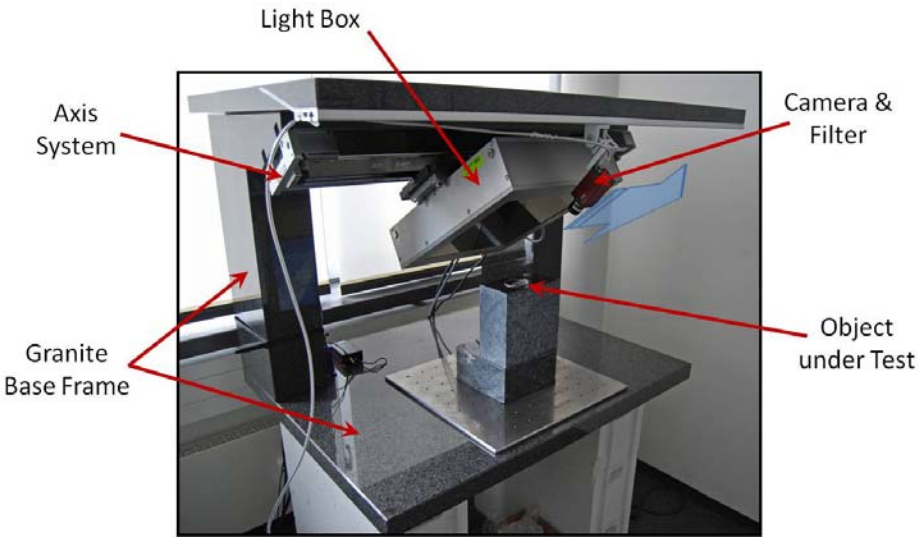

Figure 10. First prototype of a setup for UV-line-shift deflectometry[26,27]. The luminous line structures are provided using a chrome-plated quartz mask ("light box"), mounted onto a linear stage.

7. MEASUREMENT EXAMPLES

Figure 11 shows a measurement result for the curvature map of an untreated varifocal eyeglass, obtained using the setup shown in figure 10. The measurement accuracy for the local curvature (~0.01D) is comparable to the performance of a conventional PMD setup for non-transparent objects.

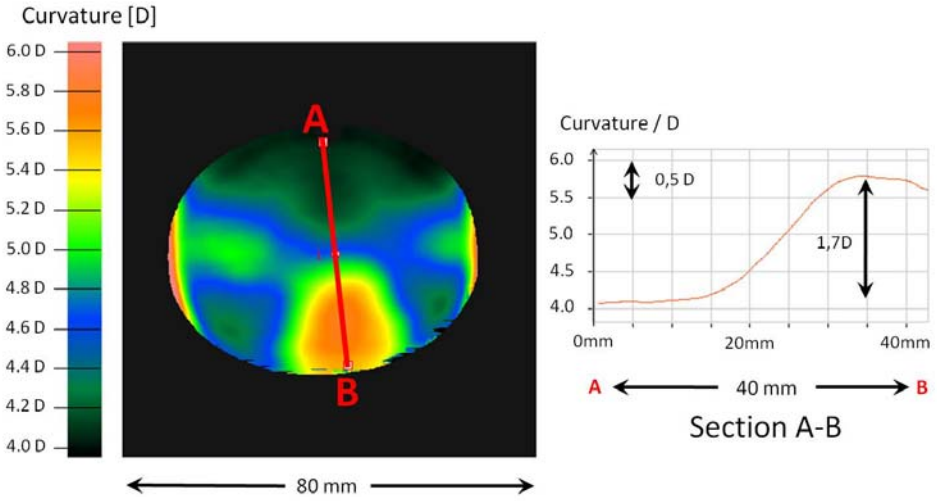

Figure 11. Curvature map of a varifocal eyeglass, obtained using the UV-line-shift setup shown in figure 10. Mind the fact that the rear surface of the specimen has not been treated in any way[27].

Deflectometry can also be used for the assessment of the performance of large astronomical mirrors. Figure 12 shows the slope deviation maps of a hexagonal mirror prototype manufactured for the Cherenkov Telescope Array project (CTA)[46]. The mirror has a diameter of 1.20m flat-to-flat and a radius of curvature of 30m. The measurement clearly shows the streak lines of the float glass sheet used as substrate as well as slope deviations in the center and at the edges of the mirror.

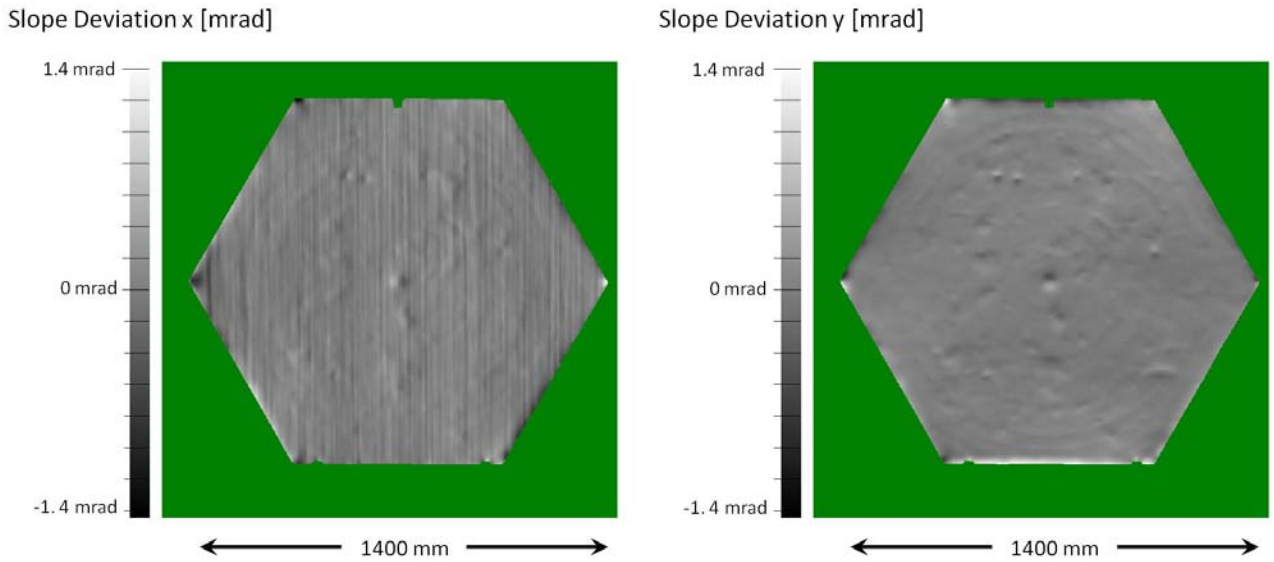

Figure 12. Slope deviation maps of a mirror prototype manufactured for the Cherenkov Telescope Array (CTA), measured by Phase Measuring Deflectometry (PMD). Left: Slope deviation in x-direction. Right: Slope deviation in y-direction. Mirror prototype courtesy of CEA Saclay[27].

The geometry data of the mirror topography obtained by the PMD measurement can also be used to determine the point spread function (PSF) of the mirror for different imaging scenarios. Figure 13 shows a comparison of the PSF at 2f, calculated from PMD measurement (left) and directly captured on a piece of paper (right).

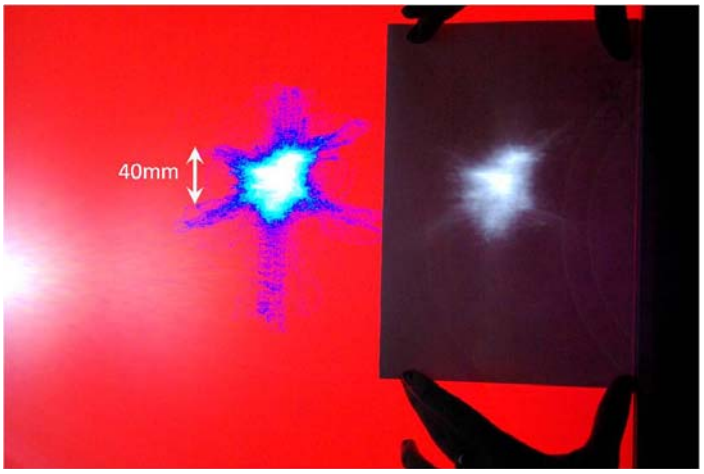

Figure 13. Comparison of the point spread function of the mirror shown in figure 12, calculated from the PMD measurement (left) and directly captured on a piece of paper (right). The calculated PSF is displayed on the screen of the PMD setup exactly at the position that was used for the measurement, applying the same pixel scaling. By placing a point light source close to the entrance pupil of the camera which had been used for the measurement, the "experimental" PSF (right) is directly imaged by the mirror (standing 30m away) onto the screen next to the calculated one with the same scaling. To enhance the low-intensity fine structure of the PSF, the photograph has been overexposed in the center, and the calculated PSF has been displayed using a log scale[27].

Finally, figure 14 shows a miniaturized PMD setup that has been developed specifically for *machine-integrated PMD measurements* within an ultraprecision diamond turning machine[47]. The setup can be mounted directly onto the B-table of the lathe, allowing for a measurement of the workpieces without releasing them from the vacuum chuck. This paves the path for a closed-loop *machine integrated correction cycle*. Figure 15 shows the comparison of the measurement results for a non-rotationally symmetric freeform workpiece, obtained by machine-integrated PMD (left) and by an external reference measurement using a ZygoLOT NewView 5010 white light interferometer (right)[48]. The considerable

difference in measurement time (~10min for PMD, ~2.5h for WLI) is due to the fact that the WLI only supports a limited measurement field of 1.8mm x 1.44mm at a lateral resolution of 5.6µm, so that the complete height map for a field of ~20mm x 20mm had to be stitched from 315 single measurements. In contrast to this, the machine integrated PMD was able to acquire the complete data set within one field of view (at a coarser lateral resolution of 25µm).

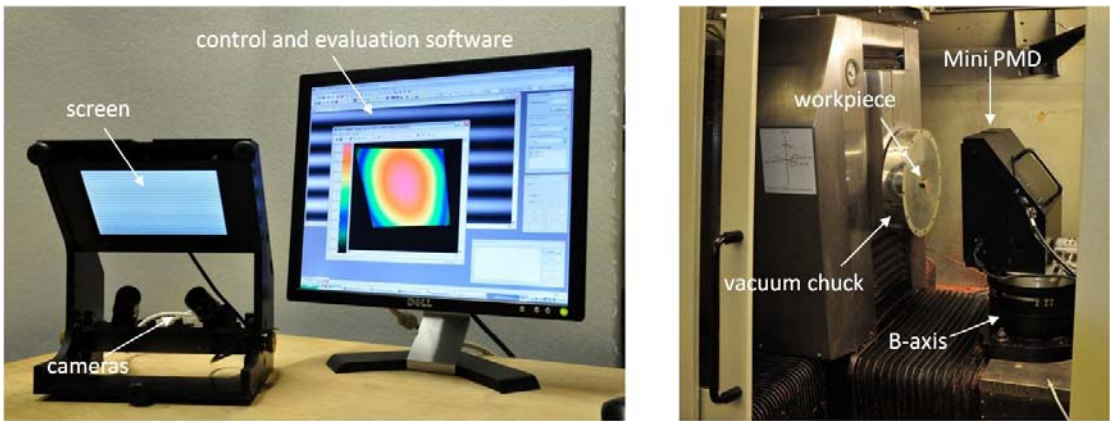

Figure 14. Miniaturized PMD setup developed for machine integrated measurements inside an ultraprecision diamond turning machine. Left: Setup with open casing. Right: Setup within the ultraprecision lathe. For the actual measurement, the setup is moved closer to the chuck, obscuring the workpiece behind the side panels to prevent stray light[27].

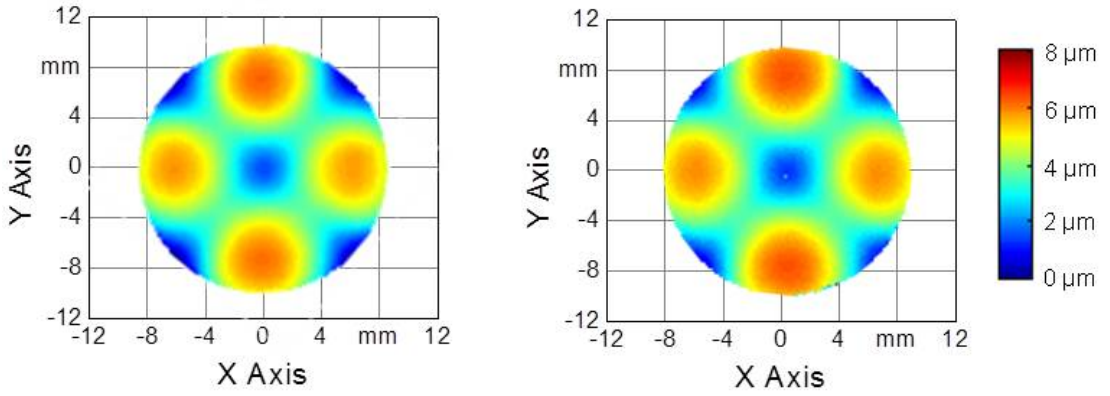

Figure 15. Comparison of the measurement of a non-rotationally symmetric freeform[27,48]. Left: Height map acquired by machine integrated PMD (measurement time ~10 min, no rechucking). Right: External measurement of the same workpiece, using a ZygoLOT NewView 5010 white light interferometer (measurement time ~2.5h with stitching). The maximum deviation between both measurements is Δ_{max}≈300nm, which is lies within the measurement uncertainty of the Mini-PMD of u=±250nm.

8. SUMMARY AND CONCLUSIONS

There are two distinct measurement principles available to optically acquire the full-field surface topography of specular objects: *interferometry* and *deflectometry.* A comparative assessment of the basic principles underlying both techniques has been given. Both the advantages and the specific shortcomings of deflectometry have been addressed and analyzed. The major drawbacks of deflectometry are the *limited global accuracy* and the perturbations caused by *parasitic reflections at the rear surface* of transparent objects. Recent developments overcoming both these limitations have been reviewed and presented.

With these developments at hand, deflectometry is now heading towards being a serious competitor for interferometry. While interferometry will probably maintain its leading position for applications with ultra high accuracy demands (i.e. uncertainties in the nanometer regime), the fact that deflectometry is now capable of measuring *arbitrary freeforms* with sub-micron accuracy *without null testing* will boost its usage for applications that up to now had been exclusively the domain of interferometry.

ACKNOWLEDGMENTS

The authors would like to thank the *Bayerische Forschungsstiftung BFS* for their financial support of the projects AZ 450/01 and AZ 748/07, as well as the *Deutsche Forschungsgemeinschaft DFG* for their financial support of the projects HA1319/11-1 and HA1319/11-2. Furthermore, we thank our collaboration partners ECAP Erlangen, CEA Saclay, IWF Berlin, 3D-Shape GmbH Erlangen, Schneider Optikmaschinen GmbH & Co. KG Steffenberg, Rupp & Hubrach Optik GmbH Bamberg, Rodenstock GmbH München, Carl Zeiss Vision GmbH Aalen, and Carl Zeiss AG Jena.

REFERENCES

[1] Creath, K., "Phase-Measurement Interferometry Techniques," in: Progress in Optics, ed. by Wolf, E., Vol. XXVI, Elsevier Science Publishers, Amsterdam, 349-393 (1988).
[2] Beyerlein, M., Lindlein, N. and Schwider, J., "Dual-wave-front computer generated holograms for quasi absolute testing of aspherics," Appl. Opt. 41, 2440-2447 (2002).
[3] Goodwin, E. P. and Wyant, J. C., [Field Guide to Interferometric Optical Testing], SPIE Press, Bellingham, WA (2006).
[4] Foucault, L.M., "Description des procédées employés pour reconnaître la configuration des surfaces optiques," Comptes rendus hebdomadaires des séances de l'Academie des Sciences 47, 958-959 (1858).
[5] Hartmann, J., "Bemerkungen über den Bau und die Justierung von Spektrographen," Zeitschrift für Instrumentenkunde 20, p.17 (1900).
[6] Shack, R. and Platt, B., "Production and Use of a Lenticular Hartmann Screen," Journal of the Optical Society of America 61, 656-660 (1971).
[7] Häusler, G., "Verfahren und Vorrichtung zur Ermittlung der Form oder der Abbildungseigenschaften von spiegelnden oder transparenten Objekten," German patent DE 19944354 (1999).
[8] Knauer, M. C., Kaminski, J., Häusler, G., "Phase Measuring Deflectometry: a new approach to measure specular free-form surfaces," Proc. SPIE 5457, 366-376 (2004).
[9] Ritter, R. and Hahn, R., "Contribution to analysis of the reflection grating method," Opt. Las. Eng. 4(1), 13-24 (1983).
[10] Petz, M. and Tutsch, R., "Optical 3D Measurement of Reflecting Free Formed Surfaces," *International Symposium of Photonics in Measurement*, VDI-Berichte 1844, VDI-Verlag, 329-332 (2002).
[11] Petz, M., Tutsch, R., "Rasterfahndung," Messen und Prüfen – Optische Messtechnik, Carl Hanser Verlag, München, Jahrg. 47, 556-558 (2002).
[12] Pérard, D., Beyerer, J., "Three-dimensional measurement of specular free-form surfaces with a structured-lighting reflection technique," Three-Dimensional Imaging and Laser-based Systems for Metrology and Inspection III, Proc. SPIE 3204, 74-80 (1997).
[13] Pérard, D., "Automated visual inspection of specular surfaces with structured-lighting reflection techniques," Fortschritt-Berichte VDI, Reihe 8, Nr. 869, VDI Verlag, Düsseldorf (2001).
[14] Bothe, T., Li, W. et al., "High Resolution 3D Shape Measurement on Specular Surfaces by Fringe Reflection," in: *Optical Metrology in Production Engineering*, Proc. SPIE Int. Soc. Opt. Eng. 5457, 411-422 (2004).
[15] Werling, S., Beyerer, J., "Automatische Inspektion spiegelnder Oberflächen mittels inverser Muster," tm - Technisches Messen 74(4), 217-223 (2007).
[16] Balzer, J., Werling, S., "Principle of Shape from Specular Reflection," Measurement 43(10), Elsevier, 1305-1317 (2010).
[17] Su, P., Parks, R. E., Wang, L., Angel, R. P., Burge, J. H., "Software configurable optical test system: a computerized reverse Hartmann test," Appl. Opt. 49(23), 4404-4412 (2010).
[18] Kammel, S., "Deflectometry for quality control of specular surfaces," tm - Technisches Messen 70(4), 193-198 (2004).
[19] Häusler, G., "Deflectometry Rivals Interferometry," Proc. ASPE Summer Topical Meeting (2005).
[20] Häusler, G., Knauer, M. C., Faber, C., Richter, C., Peterhänsel, S., Kranitzky, C., Veit, K., "Deflectometry Challenges Interferometry: 3D Metrology from Nanometer to Meter," Frontiers in Optics, OSA Technical Digest (CD), paper FWV1 (2009).
[21] Knauer, M. C., Richter, C., Hybl, O., Kaminski, J., Faber, C., Häusler, G., "Deflektometrie macht der Interferometrie Konkurrenz," tm - Technisches Messen 76(4), 175-181 (2009).

[22] Olesch, E., Faber, C., Seraphim, M. C. and Häusler, G., "New Holistic Self-Calibration Method for Deflectometric Sensors," Proc. DGaO 111, P33 (2010).
[23] Olesch, E., Faber, C. and Häusler, G., "Object Reconstruction by Deflectometry," Proc. DGaO 113, P28 (2012).
[24] Faber, C., Knauer, M. C and Häusler, G., "Can deflectometry work in presence of parasitic reflections?" Proc. DGaO 110, A10 (2009).
[25] Faber, C., Seraphim, M. C., Sprenger, D. and Häusler, G., "Algorithmic Elimination of Parasitic Reflections in Deflectometry," Proc. DGaO 111, A18 (2010).
[26] Sprenger, D., Faber, C., Seraphim, M. C. and Häusler, G., "UV-Deflectometry: No parasitic reflections," Proc. DGaO 111, A19 (2010).
[27] Faber, C., "New Methods and Advances in Deflectometry," PhD thesis, Friedrich-Alexander-University of Erlangen-Nuremberg (2012, to be published).
[28] Malacara, D., [Optical Shop Testing], Wiley Series in Pure and Applied Optics, Wiley-Interscience, 3rd edition (2007).
[29] Bruning, J. H., "Fringe Scanning Interferometers," in: Optical Shop Testing, ed. by Malacara, D. M., John Wiley & Sons, 409-437 (1978).
[30] Koliopoulos, C. L., "Interferometric Optical Phase Measurement Techniques," PhD thesis, The University of Arizona (1981).
[31] Küchel, M. F., "Interferometric measurement of rotationally symmetric aspheric surfaces," Proc. SPIE 7389, 16-34 (2009).
[32] Garbusi, E., Pruss, C., Osten, W., "Interferometer for precise and flexible asphere testing," Optics Letters 33(24), 2973-2975 (2008).
[33] Häusler, G. and Schneider, G., "Testing optics by experimental ray tracing with a lateral effect photodiode," Appl. Opt. 27(24), 5160-5164 (1988).
[34] Ehret, G., Schulz, M., Baier, M., Fitzenreiter, A., "A new optical flatness reference measurement system," Proc. DGaO 110, P22 (2009).
[35] Photonic Metrology GmbH & Co KG, "Photonic Metrology - RaySense," <http://www.photonic-metrology.com/produkte/RaySense/index.html> (2012).
[36] Horneber, C., "Phasenmessende Deflektometrie – ein Verfahren zur hochgenauen Vermessung spiegelnder Oberflächen," PhD thesis, University of Erlangen-Nuremberg, 12-13 (2006).
[37] Werling, S, "Deflektometrie zur automatischen Sichtprüfung und Rekonstruktion spiegelnder Oberflächen," PhD thesis, Schriftenreihe Automatische Sichtprüfung und Bildverarbeitung, Vol. 3, KIT Scientific Publishing, Karlsruher Institut für Technologie, 46-72 (2011).
[38] Knauer, M. C., Häusler, G., Lampalzer, R., "Verfahren und Vorrichtung zur Bestimmung der Form und der lokalen Oberflächennormalen spiegelnder Oberflächen," German patent DE 102004020419 (2004).
[39] Knauer, M. C., Kaminski, J. and Häusler, G., "Absolute Phasenmessende Deflektometrie," Proc. DGaO 105, A15 (2004).
[40] Knauer, M. C., "Absolute Phasenmessende Deflektometrie," PhD thesis, Friedrich-Alexander-University of Erlangen-Nuremberg (2006).
[41] Sessner, R., Häusler, G., "Richtungscodierte Deflektometrie," Proc. DGaO 105, A16 (2004).
[42] Sessner, R.., "Richtungscodierte Deflektometrie durch Telezentrie," PhD thesis, Friedrich-Alexander-University of Erlangen-Nuremberg (2009).
[43] Balzer, J., Werling, S., Beyerer, J., "Regularization of the deflectometry problem using shading data," Proc. SPIE 6382, 63820B (2006).
[44] Kaminski, J., "Geometrische Rekonstruktion spiegelnder Oberflächen aus deflektometrischen Messdaten," PhD thesis, Friedrich-Alexander-University of Erlangen-Nuremberg, 22-55 (2008).
[45] Schwider, J., Burow, R. et al, "Digital wave-front measuring interferometry: some systematic error sources," Appl. Opt. 22(21), 3421-3432 (1983).
[46] Krobot, R, Faber, C., Olesch, E., Häusler, G., Schulz, A., Stinzing, F., Stegmann, C., "Deflectometric Measurement of 10,000 Telescope Mirror Tiles," Proc. DGaO 112, P27 (2011).
[47] Röttinger, C., Faber, C., Olesch, E., Häusler, G., Kurz, M., Uhlmann, E., "Deflectometry for Ultra Precision Machining – Measuring without Rechucking," Proc. DGaO 112, P28 (2011).
[48] Faber, C., Kurz, M., Röttinger, C., Olesch, E., Domingos, D., Löwenstein, A., Häusler, G., Uhlmann, E., "Two Approaches to use Phase Measuring Deflectometry in Ultra Precision Machine Tools," Proc. Euspen 12 Vol. 2, 84-87 (2012).